British Journal of Applied Science & Technology
11(3): 1-14, 2015, Article no.BJAST.17663
ISSN: 2231-0843

SCIENCEDOMAIN *international*
www.sciencedomain.org

The Edge Effect on the EEDF Measurements of Magnetized DC Plasma

A. R. Galaly[1,2*] and M. A. Khedr[3]

[1]Department of Environment and Health Research, the Custodian of the Two Holy Mosques Institute for Hajj and Umrah Research, Umm Al-Qura University, Makkah, P.O.Box 6287, KSA.
[2]Department of Physics, Faculty of Science, Beni-Suef University, Egypt.
[3]National Institue of Laser Science, Cairo University, 12613 Giza, Egypt.

Authors' contributions

This work was carried out in collaboration between both authors. Author ARG designed the study, performed the statistical analysis, wrote the protocol and wrote the first draft of the manuscript and managed literature searches. Authors ARG and MAK managed the analyses of the study and literature searches. Both authors read and approved the final manuscript.

Article Information

DOI: 10.9734/BJAST/2015/17663
Editor(s):
(1) David G. Yurth, Director: Science & Technology, The Nova Institute of Technology Holladay, Utah, USA.
(2) Mark Vimalan, Department of Physics, Syed Ammal Arts and Science College, India.
(3) Selvakumar Subbian, Laboratory of Mycobacterial Pathogenesis and Immunity, Public Health Research Institute (PHRI) at Rutgers Biomedical and Health Sciences, Newark, USA.
Reviewers:
(1) Anonymous, University of Belgrade, Serbia.
(2) Anonymous, Universiti Teknologi PETRONAS, Malaysia.
(3) Anonymous, CIMAV, Mexico.
Complete Peer review History: http://sciencedomain.org/review-history/10583

Review Article

Received 23rd March 2015
Accepted 9th July 2015
Published 16th August 2015

ABSTRACT

The localized plasma parameters at the edge of the discharge electrodes cell have been investigated for axial distribution, such as the electric field distribution, the electron energy distribution functions (EEDF), the electron temperature (T_e) and the electron density (N_e), all have been determined with and without the applications of external magnetic field using Langmuir single probe in the three regions of the discharge. The EEDF was investigated using two different methods e.g. the graphical method and the electron current second derivative method. The electron energy distribution functions are maxwellian only in the positive column region (P.C.) and non- maxwellian in the cathode fall (C.F) and the negative glow (N.G.) regions, where two groups of electrons were observed. The diffusion coefficients and the electron temperatures are lower in the presence of the magnetic field, where T_e decreased from 6.5 to 3 eV for C.F, from 5.18 to 2.6

**Corresponding author: E-mail: ahmed_galaly@yahoo.com;*

eV for N.G., and from 4.2 to 1.1 eV for P.C. Furthermore, sharp axial increments for potential distribution and electron density in the presence of the magnetic field were measured, whereas in the border between C.F and N.G regions, N_e increased from 4 x10^9 to 9.5 x10^9 cm^{-3} and 4.97 x10^9 to 11.6 x10^9 cm^{-3}, respectively. In contrast, an axial decrement of the electron density in P.C. region due to the electron capture by the anode in P.C. region was also found.

Keywords: Single langmuir probe; electron energy distribution function; Maxwellian energy distribution; edge effect.

PACS No.: 52.50.-b.

1. INTRODUCTION

The electron energy distribution function (EEDF), in most plasma diagnostic techniques, is usually assumed to be Maxwellian. However it is of interest to verify this assumption which helps also for explain the mechanism of the glow discharge in the different discharge regions (i.e.:- cathode fall, negative glow and positive column regions) [1-2] among the different diagnostic techniques there are the method of Langmuir probes. Basically, an electrostatic probe is merely a small metallic electrode inserted into the plasma. By assuming a maxwellian velocity distribution, plasma parameters e.g. the electron temperature and electron density can be determined from the current-voltage (I-V) characteristic curve of the probe. The electric probe method has one advantage over all other diagnostic techniques; since it produces local measurements for the different regions in the discharge volume [3].

The plasma is considered to be a quasi-neutral. This quasi-neutrality is, however, distributed by introducing the probe into the plasma. A sheath is formed around the conducting surface of the probe due to the redistribution of charges. However, the bulk of the plasma can be considered to be undisturbed outside the sheath, which is usually very thin. The motion of electrons and ions near the probe are dependent on the polarity as well as the amplitude of the probe potential relative to the plasma potential. When the probe potential is sufficiently negative; only the ions can reach the probe surface. The current is thus equal to the ion random current (I_{ri}) [4].

Kagan and Perel [5] showed that the magnetic field does not disturb the I – V characteristic of a cylindrical Langmuir probe, if the probe radius is too small relative to the electron Larmor radius, and it is placed perpendicular to the magnetic field lines. By using the optical emission spectroscopy and a collisional-radiative model, the non-maxwellian electron energy distributions in low-pressure plasmas can be determined. Furthermore determination of the electron temperature and density in the negative glow of a nitrogen pulsed discharge using optical emission spectroscopy [6-7].

In the present work, the edge effect on the EEDF measurements of magnetized dc argon plasma is investigated in the different discharge regions using a single spherical probe. Two methods are used to investigate the energy distribution namely: The semi-log curve of the electron current and the second derivatives of the electron current method. Furthermore electron energy distribution function, electron density, and temperatures measurements are carried out.

2. EXPERIMENTAL SETUP

Details of the experimental setup and procedures of the work are shown in our previous work [8]. In this study, an electric single probe [9] inserted into the plasma, and a potential V_P is applied to the probe. The basic single probe electric circuit is shown in Fig. 1a.

A single spherical probe of 2 mm diameter, made of phosphor bronze was used. The probe diameter was as small as possible to avoid, or at least to minimize, the disturbing influence of its tip on the plasma. The probe was also cleaned, to reduce the surface contamination effects, by electron bombardment. The electron bombardment of the probe was done by connecting it to a steady positive voltage between 60-100 volts. The electrical circuit used for the single probe consists of a DC-power supply, 10 turns potentiometer (50 K Ω), the load resistor (Rp = 1K Ω) and a 10 μF capacitor. The 10 μF capacitor was placed in parallel with the measuring resistor Rp to filter out the noise. The geometry and the dimension of the used magnet are shown in Fig. 1b.

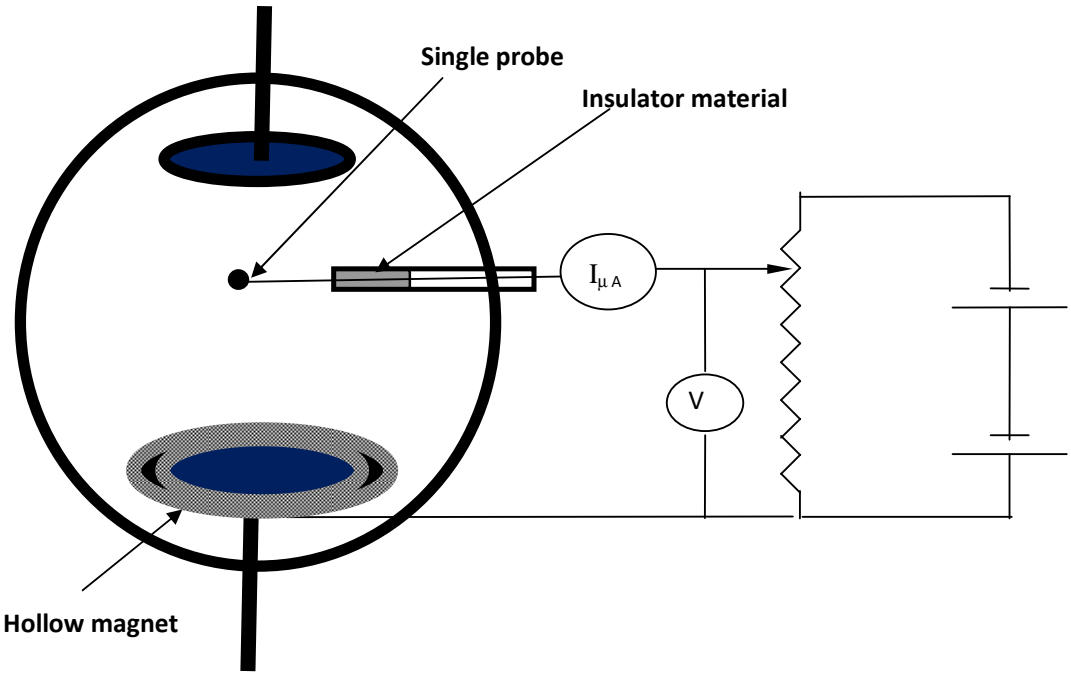

Fig. 1a. The single probe circuit

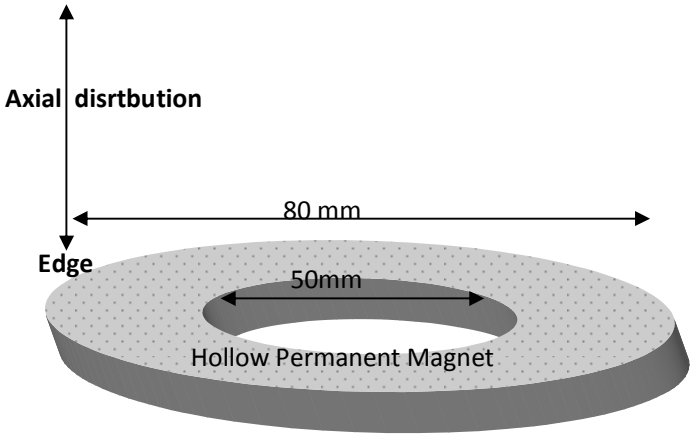

Fig. 1b. Axial distribution for the magnetic field strengths

3. RESULTS AND DISCUSSION

3.1 Axial Distribution of the Magnetic Field Strength at Edge

Edge of the cathode is our interested fashion region more than the center due to the strong hollow permanent magnet around the cathode, so the effect of the magnetic field at the center is lower than at the edge [10], therefore the electrons are trapped by magnetic field lines at the edge more than at the center, moreover, the space charge density increases, and the electric field values increases due to the increase of the potential values [11]. Fig. 2 shows that the magnetic field strength (B) at the edge has its maximum value in the cathode fall region (B=400 gauss) and begin to decrease in the axial direction towards the positive column (B=350 gauss), passing through the negative glow region.

3.2 The Electric Field Distribution

Values of the electric field are obtained by differentiate the measured potential distribution

curves i.e. (E = dV/dX). Fig. 3 shows the electric field distribution for Ar - discharge, at different gas pressures (1- 4 mbar) and 10 mA discharge current.

The electric field decreased sharply along the cathode – anode space. This is related to the intense positive space charge in the front of the cathode which accelerates the electrons towards the anode. Thus, the electrons emitted from the cathode are then accelerated away until they reach the negative glow region where the electric field becomes weak (zero and sometimes negative values). In this region, the gained kinetic energy of the electrons is dissipated in collisions with the atoms of the gas and thus secondary electrons would be produced [12]. In the positive column region, constant and linear electric field is needed to maintain the discharge along the large length of the column which is required to carry the discharge current.

Fig. 4 shows the electric field distribution for Ar discharges in the presence of magnetic fields which are similar to the distribution without magnetic field, although values of the electric field distribution at the edge are higher by a factor of (2-1.5) in the pressure range of (1-4 mbar) at the cathode side and in the negative glow region.

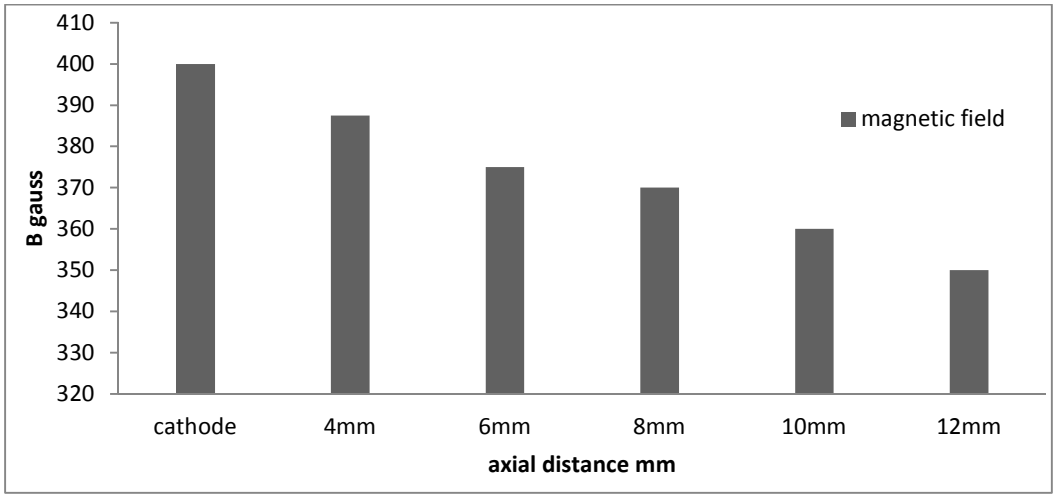

Fig. 2. Axial distribution of the magnetic field strength

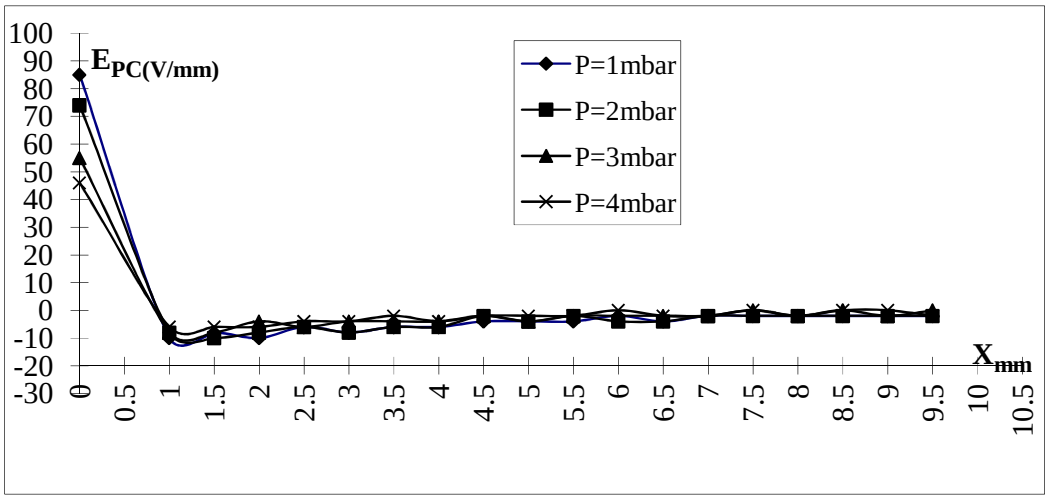

Fig. 3. Axial electric field distribution in at edge in the absence of magnetic field at constant current (I=10 mA)

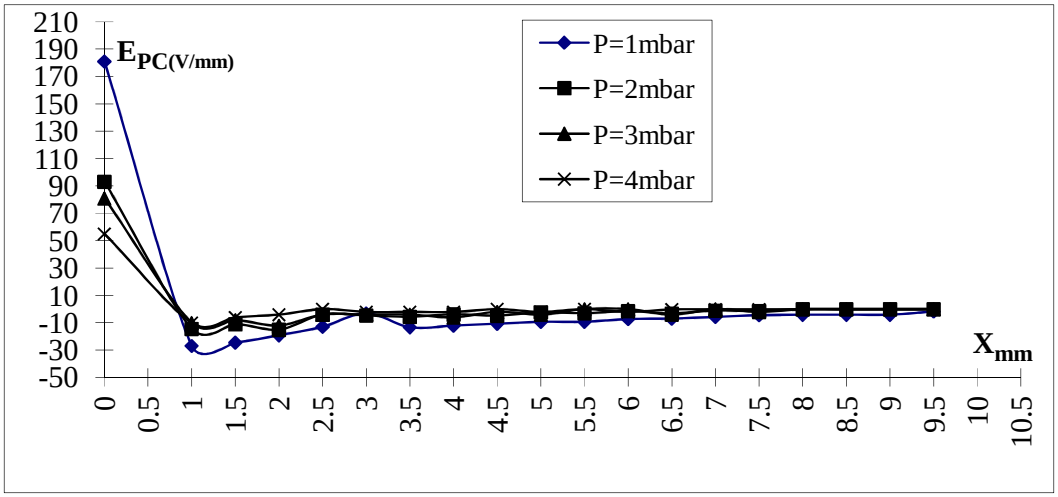

Fig. 4. Axial electric field distribution in the presence of magnetic field at current I=10 mA (at the edge)

3.3 The (Ia-Va) Characteristic of the Single Probe

The I-V characteristic curves produced useful information about the electron energy distribution function, electron temperature and electron density. Figs. 5 and 6, show i-v characteristic curves of the single probe at edge in the cathode fall region, at different pressures, in the presence and the absence of the magnetic field for Ar discharge.

When the magnetic field is applied, the diffusion coefficient of the electron $D_{\perp}$ is reduced due to following equation [13]

$$De_{\perp} = \frac{De}{1 + \omega^2 \tau^2} \quad (1)$$

Where D_e is the electron diffusion coefficient

$$D_e = KT/m_e \nu_{\pi} \quad (2)$$

Where KT is the particle temperature in eV, ν_p is the langumer plasma frequency in Hz, where

$$\nu_p = \frac{1}{2\pi}\sqrt{\frac{ne^2}{m_e \varepsilon_0}} \quad (3)$$

m_e and n are mass and density of electron respectively.

Consequently $De_{\perp}$ is reduced by a factor of [1/ [1 + $(\omega\tau)^2$]. here ω is the cyclotron frequency of the electron and τ is the mean free time of the electron-atom collision, $\omega = \frac{eB}{m}$. Although the current and current density increases in the presence of the magnetic field, the rate of plasma loss by diffusion must decrease in the presence of magnetic field [14].

3.4 EEDF Measurements in the Cathode Fall and Negative Glow Regions

3.4.1 Using the semi-log curve of the electron current method

The first method depends on the plotting of the semi-log curve of the electron current. I_e as a function of the probe voltage V_P. For a maxwellian energy distribution, a straight line with a slope of $(\frac{-e}{K T_e})$ is expected. A departure from linearity, however, doesn't necessarily mean that the distribution is not maxwellian. The departures from linearity could also be caused by a spread in the work function over the surface of the probe, adrift in the work function of the probe can be related to the finite probe size and the fluctuations of electron temperature [15].

Figs. 7a, b and c, show the semi-log curves of the electron current for the different glow discharge regions:- Cathode fall and negative glow and positive column respectively of Ar discharge. The discontinuity in the semi-log curves may represent the space potential $V_{s.}$ this is the point at which the electron saturation current starts in an ideal I-V characteristic of a single probe. At this potential, the collector

receives the random electron and positive ion currents. The electron current, I_e in the retarding region ($V_p < 0$) is given by:-

$$I_e = I_0 \exp\left(\frac{-eV_p}{KT_e}\right) \quad (4)$$

where V_p is the probe potential equal to ($V-V_s$) with respect to the sheath edge, V is the applied potential and V_s is the space potential. When the probe potential reaches the space potential, the current I is equal to a constant value and a horizontal line is obtained. At this point the electron current derivatives with respect to a probe voltage are equal to zero. in practical, secondary effects like reflection from the probe surface may prevent the horizontal line from being obtained. Nevertheless, the straight line in themselves are insufficient to prove the presence of maxwellian distribution. Mott-swith and langmuir [16-17] found that, a straight line may also be obtained when a beam of electrons having a common drift velocity is superimposed on maxiwellian distribution of a relatively low temperature.

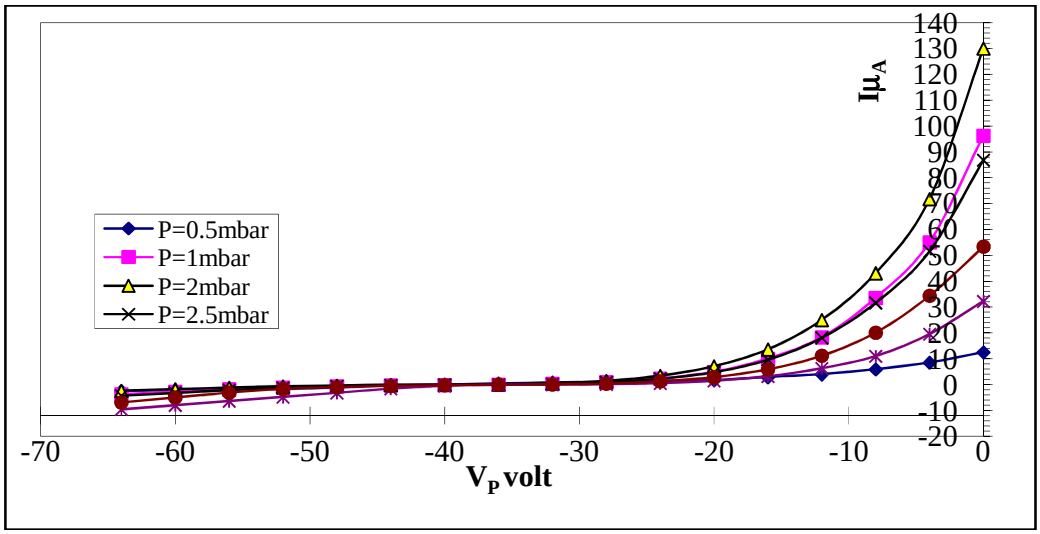

Fig. 5. I-V curves of the single probe for cathode fall region at different Ar pressures in the absence of the magnetic field (at the edge)

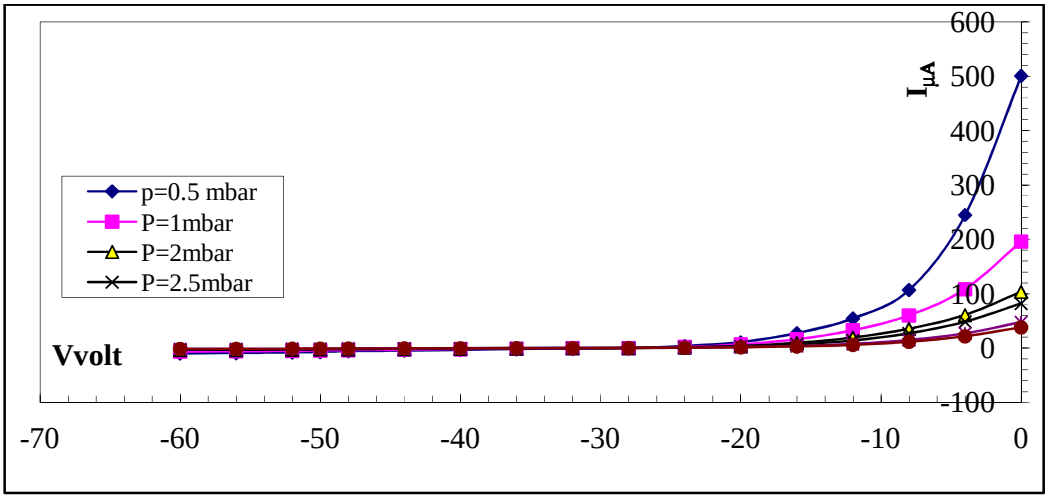

Fig. 6. I-V curves of the single probe for cathode fall region at different Ar pressures in the presence of the magnetic field (at the edge)

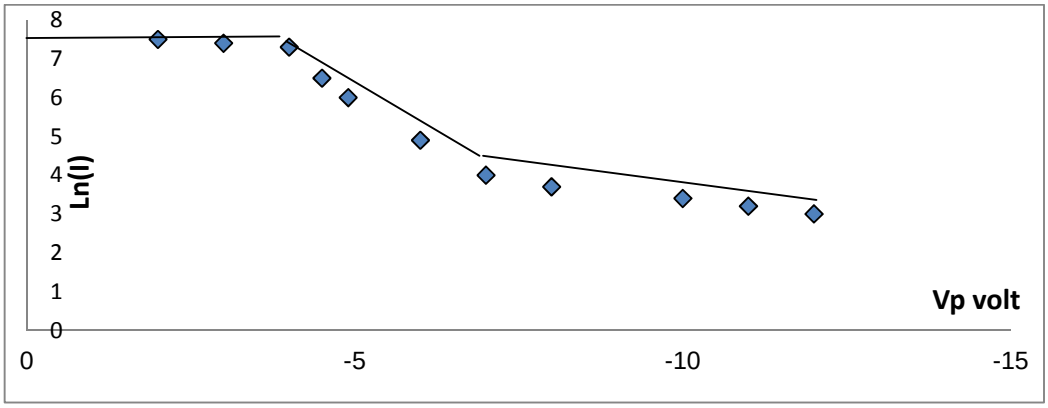

Fig. 7a. Semi-log curve of the electon current for cathode fall region

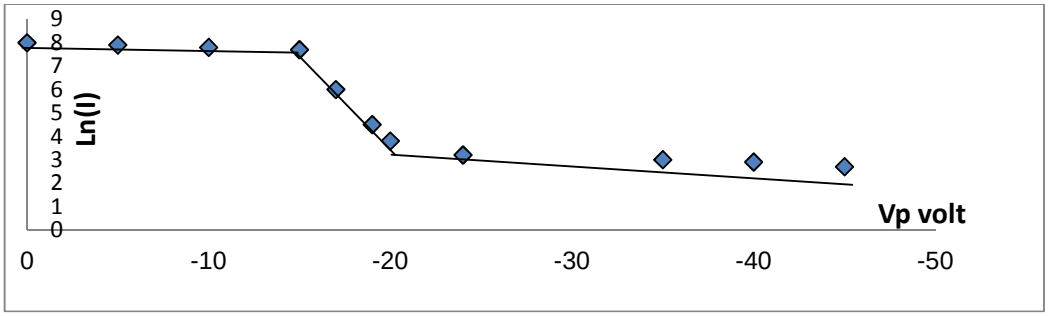

Fig. 7b. Semi-log curve of the electon current for negative glow region

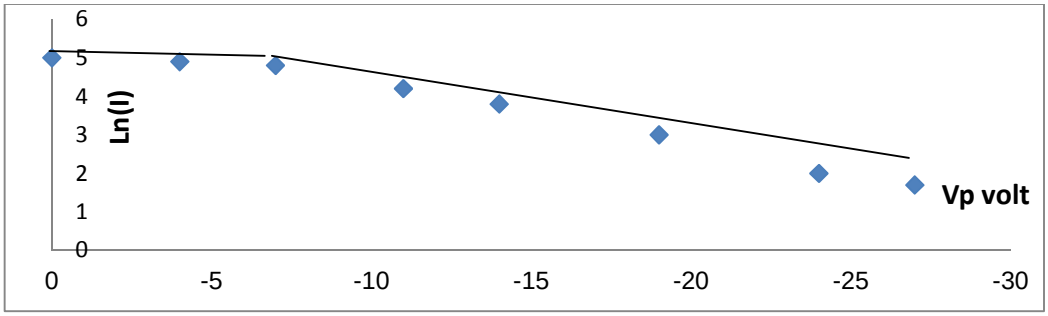

Fig. 7c. Semi-log curve of the electon current for Postive column region

3.4.2 The second derivatives of the electron current method

The second method depends on measuring the second derivatives of the electron current $\frac{d^2 I_e}{d V_P^2}$.

The energy distribution may be obtained using the relationship [18]:-

$$F(\varepsilon) = -\frac{4}{e^2 A_P}\left(-\frac{m_e V_P}{2e}\right)^{1/2}\frac{d^2 I_e}{dV_P^2} \qquad (5)$$

The second derivative was estimated by differentiate the probe current I_e twice. The EEDF was thus calculated at different gas pressure and in the different glow discharge regions. The measured electron energy distribution functions were compared with the theoretical maxwellian distribution function. The latter was computed using the relationship:-

$$F(\varepsilon) = Const.\,(\varepsilon_P)^{1/2}.\exp\left(\frac{-\varepsilon_P}{K T_e}\right) \qquad (6)$$

Where ε is the electron energy, and the presence of maxwellian distribution was tested by plotting the semi-log curves of the second derivative, against V_p . Equations (5) and (6) confirm that a plot of $\ln(\frac{d^2 I_e}{d V_p^2})$ as a function of V_p would produce a straight line having a slope of $(\frac{-e}{K T_e})$ whenever the distribution is maxwellian.

This method is the more sensitive test for the Maxwellian distribution function. By drawing the second derivative $Y'' = (\frac{d^2 I_e}{d V_p^2})$ as shown in Figs. 8a, b and c, as a function of the probe voltage v_p . Then the semi-log curves of the second derivative of the electron current $\ln(\frac{d^2 I_e}{d V_p^2})$ as a function of the probe voltage v_p can be calculated. two linear parts are shown in Figs. [9a and b], which related to the existence of two groups of electrons of different temperature [19], while a straight line, Fig. 9c, is related to one group of electrons.

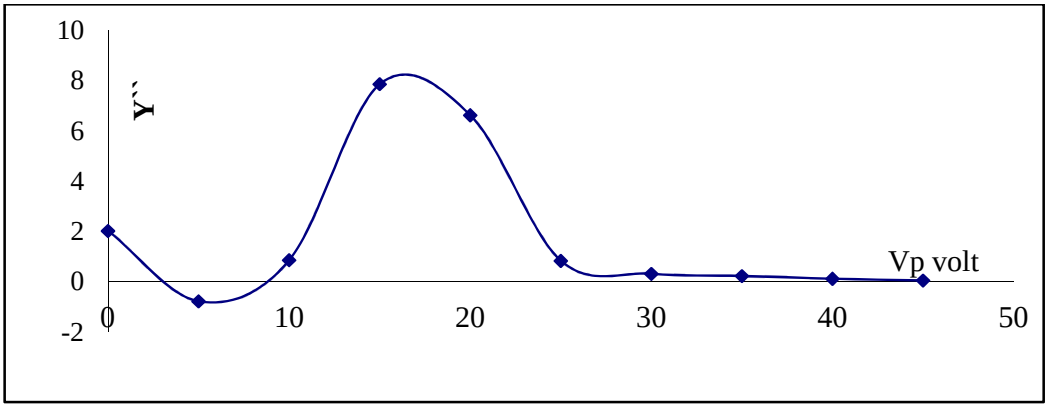

Fig. 8a. The second derivative of the electron current for cathode fall

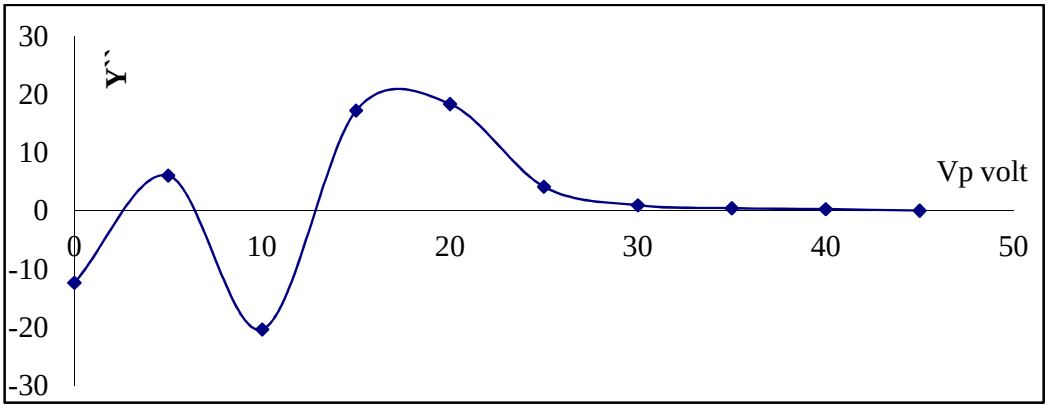

Fig. 8b. The second derivative of the electron current for negative glow

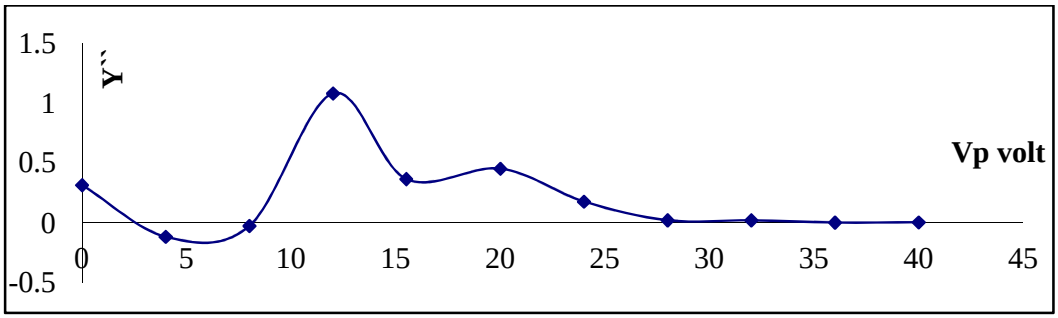

Fig. 8c. The second derivative of the electron current for postive column

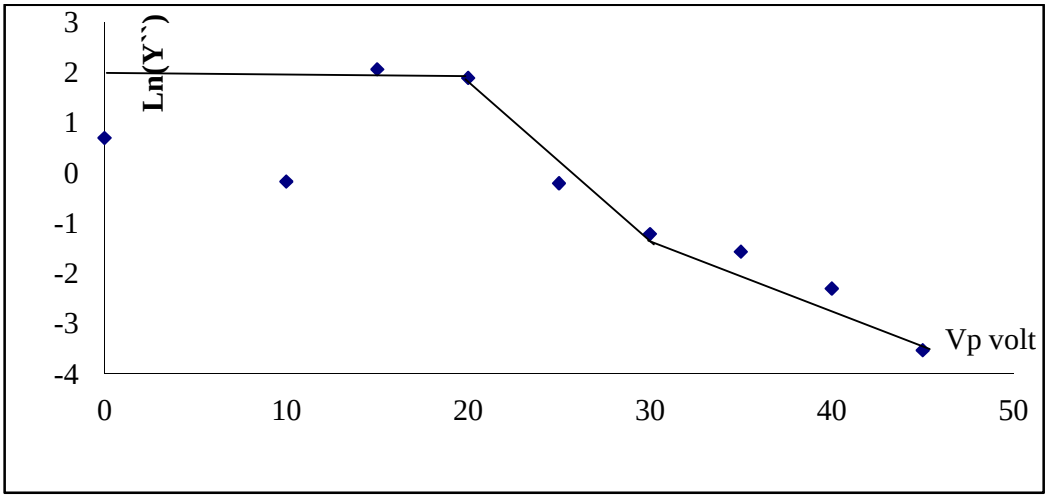

Fig. 9a. Semi-Log curve of the second derivative of the electron current for cathode fall

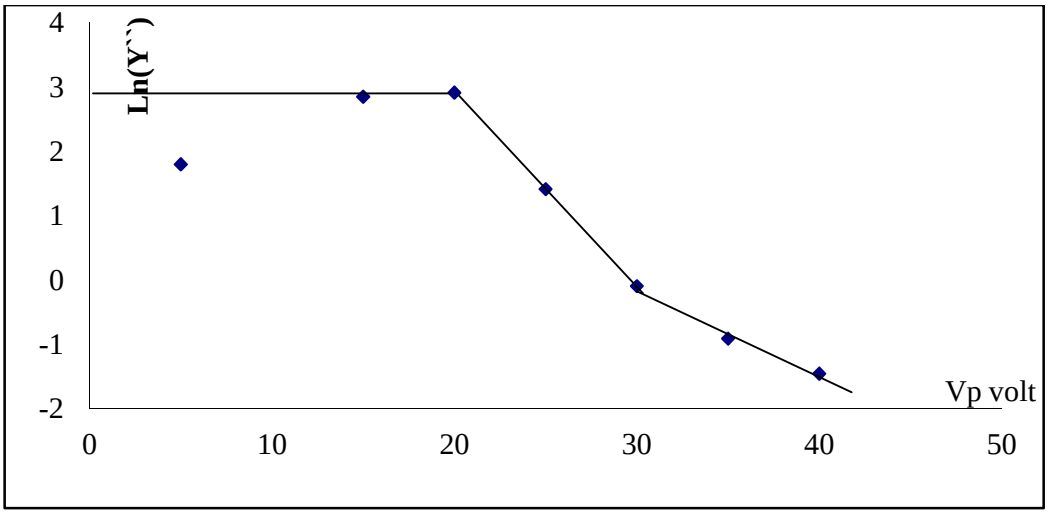

Fig. 9b. Semi- log of the second derivative of the electron current for negative glow

3.4.3 Electron energy distribution function measurements

The electron energy distribution function F(E) was thus calculated using equation (5). Figs. [10a, b and c] show f(E) as a function of the probe retarding potential V_p (which can be considered as the electron energy). Two well-defined maxima are observed for Ar glow discharge. The presence of two groups of electrons at the edge of the cathode fall and in the negative glow region can be explained as follows:-

The secondary group of electrons is those which have been ejected after collision between the fast primaries and gas atoms, and that they have not had time to reach thermal equilibrium with the ultimate group “slowest group of electrons" which has the highest number density, and are produced by the degeneration of primary and secondary groups in successive collision to very low energies, before removal by diffusion to the walls [20]. Moreover, the state of non-equilibrium between the electrons and the electric field gives rise to a non-maxwellian electron energy distribution in both cathode sheath and negative glow regions. Three distinct groups of electrons were detected:-

(I) Primary electrons from the cathode that pass through the cathode sheath region without collisions.

(II) Secondary electrons corresponding to the tail of the flux distribution with energies greater than the ionization potential.
(III) Ultimate slow electrons with energies blew the ionization potential.

The effect of magnetic field in the three glow regions C.F., N.G. and P.C. give the same behavior and trends of the previous curves:- The semi-log curve of the electron current, the second derivatives of the electron current, and the electron energy distribution function measurements but with different slopes of straight lines to give a vital change for the values of electron temperatures and densities.

3.4.4 The electron temperature and density measurements

The cathode fall region (C.F.), in the absence of the magnetic field, values of T_e varied from 6.5 to 4.5 eV, and values of N_e varied from (4 to 3) $x10^9$ cm^{-3}. In the presence of the magnetic field, T_e varied from 3 to 2 eV and N_e varied from (9.5 to 7.5) $x10^9$ cm^{-3}. For negative glow region (N.G.), without magnetic field, T_e values varied from 5.18 to 4.45 eV, and values of N_e varied from (4.97 to 4.3) $x10^9$ cm^{-3}. In the presence of the magnetic field, T_e varied from 2.6 to 2 eV and N_e from (11.6 to 8.9) x 10^9 cm^{-3}. Electrons emitted from the cathode surface were accelerated through the cathode fall edge and enters the negative glow region. They lose some of their energy in collisional excitation processes. The length of the negative glow region is then determined by dissipation of the electron energy due to inelastic collisions with neutral atoms [21]. For Positive Column Region (P.C.), in the absence of the magnetic field values of T_e, varied from 4.2 to 3.7 eV, and N_e were (5.98 to 5.66) $x10^9$ cm^{-3}, and in the presence of the magnetic field, varied from 2.5 to 1.1 eV and N_e were (5.2 to 4.55) x 10^9 cm^{-3}.

Fig. 11a shows a sharp axial decrement of the electron temperatures in the presence of the magnetic field from the C.F. region to the P.C. passing through the N.G. region. This may be attributed to the influence of the magnetic field acts as the effect of increasing the rate of ionization by increasing the pressure and consequently, increasing in the number of electron-atom collisions.

Fig. 11b shows a sharp axial increment of the electron density in the presence of the magnetic field from the cathode fall region to the negative glow region is related to the confinement of plasma in cathode fall and negative glow regions then more excitation and ionization, and a decrements of the electron density in the positive column region due to the electron capture by the anode in the positive column region.

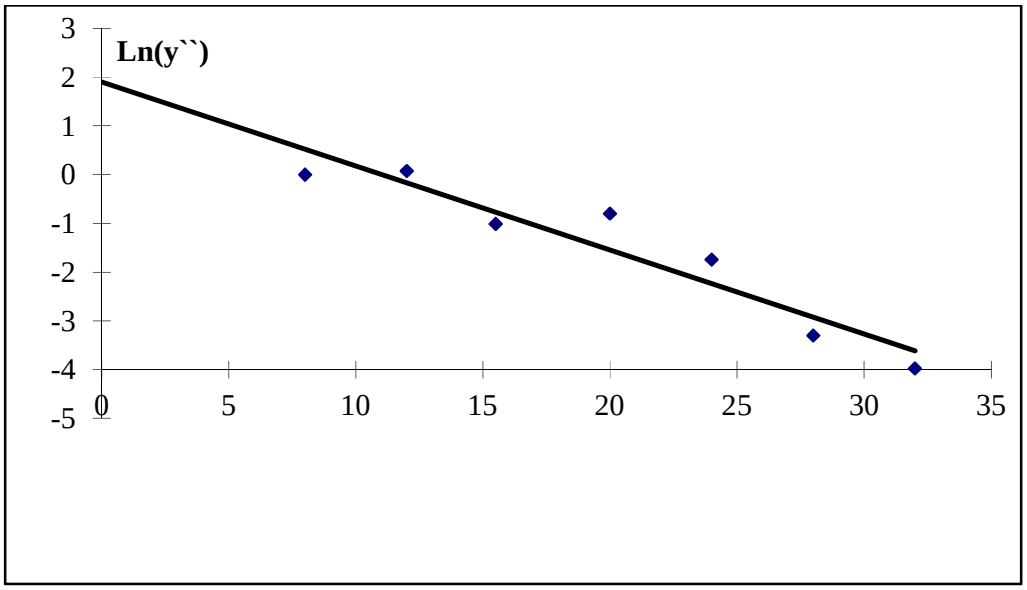

Fig. 9c. Semi- log of the second derivative of the electron current for positive column

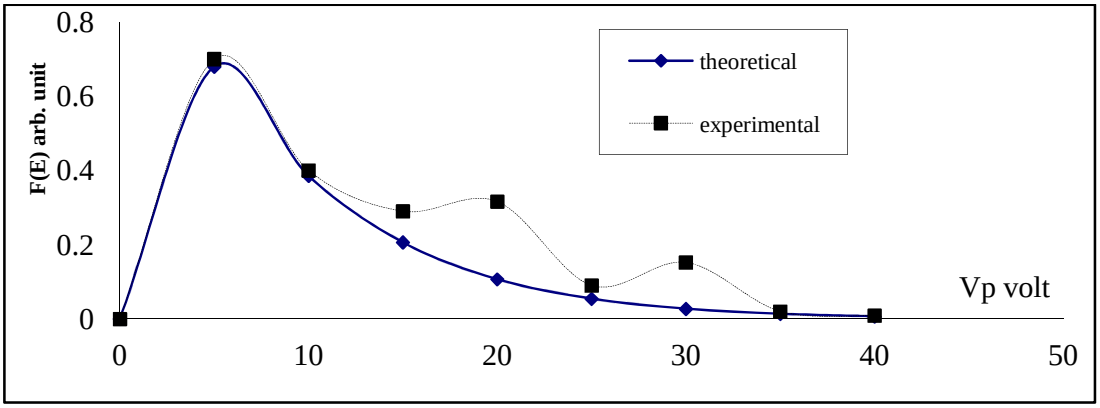

Fig. 10a. Comparison between the experimental and theortical of EEDF for cathode fall

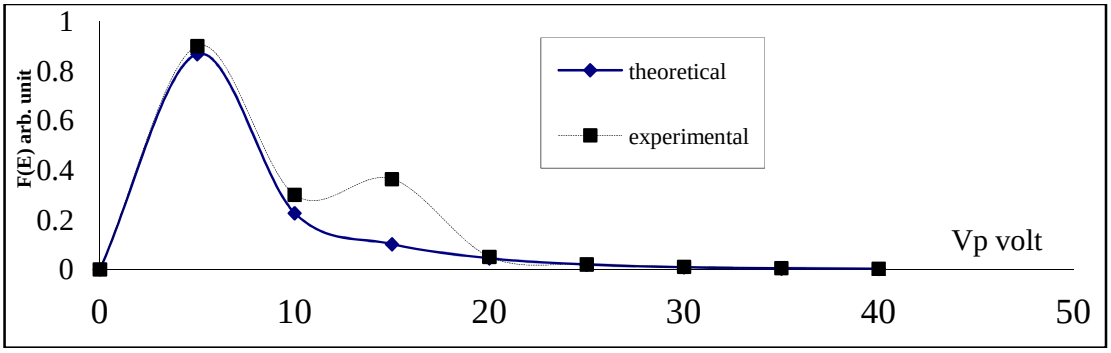

Fig. 10b. Comparison between experimental and theoretical of EEDF for negative glow

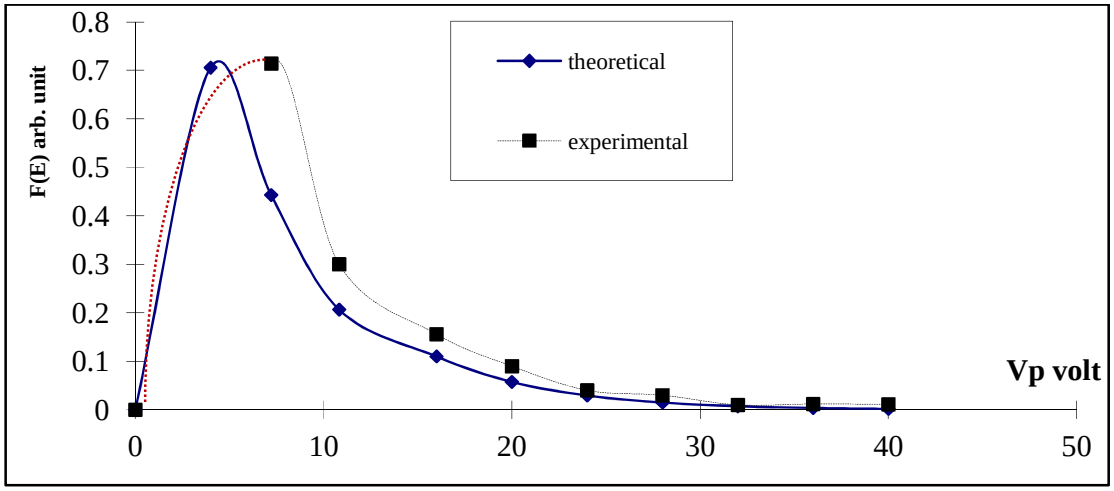

Fig. 10c. Comparison between experimental and theoretical of EEDF for positive column

All previous values show that the temperature values reduced from cathode fall to the positive column passing through the negative glow region, taking into consideration that the trend of T_e and N_e values are inversely proportional (T_e x N_e = constant) [22-23]; the maximum value of one is found where the minimum value of the other.

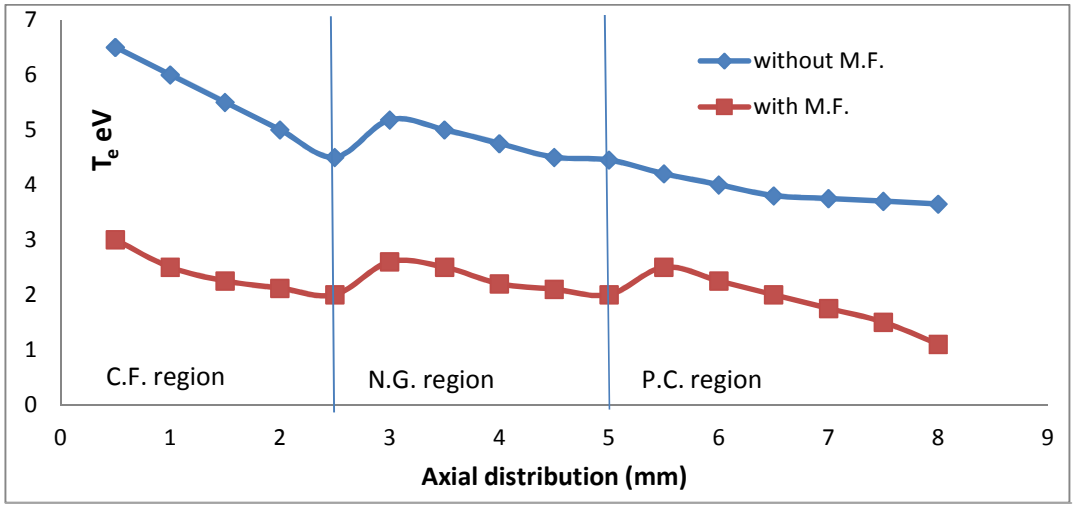

Fig. 11a. Axial distribution of electron temperatures in the presence and in the absence of magnetic field (at the edge)

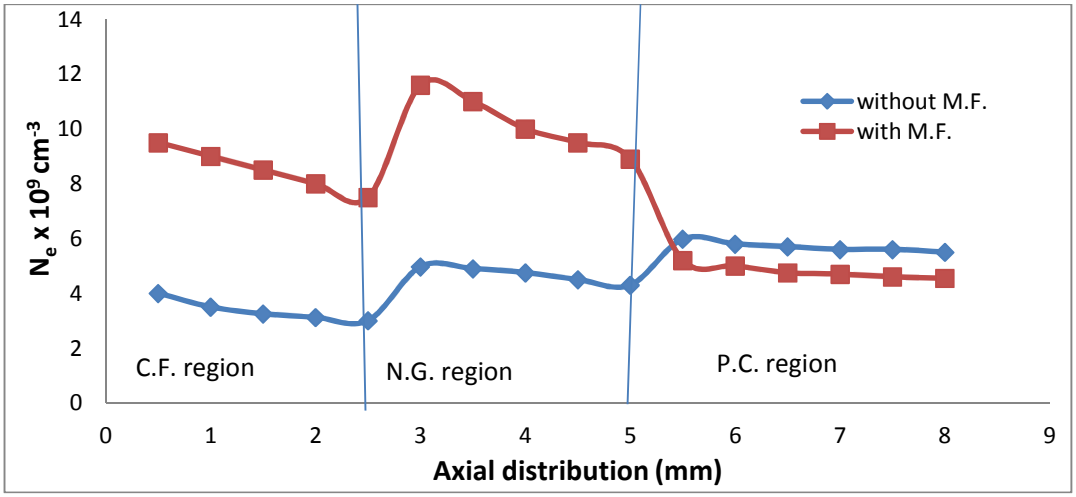

Fig. 11b. Axial distribution of the electron densities in the presence and in the presence of magnetic field (at the edge)

4. CONCLUSION

Curves confirmed that the electric discharge was mainly in the abnormal glow discharge region (I_a = 10 mA) in the pressure range of (0.5-4 mbar). The axial electric field distribution confirmed the presence of the higher field in the cathode fall region, which decreases sharply towards the negative glow and the positive column regions. In the positive column region, the electric field was weak and nearly constant. The strong electric field in the cathode fall region accelerates the electrons inward the glow discharge.

Also, it is concluded that, in the cathode fall and the negative glow regions, two groups of electrons were found. The presence of the two groups of electrons was attributed to electrons which have been ejected after the collision between the fast primaries and gas atoms. They did not had enough time to reach thermal equilibrium with the ultimate group “slowest group of electrons, which has the highest number density, and are produced by the degeneration of primary and secondary groups in successive collision to very low energies, before removal by diffusion to the walls.

On the other hand, the thermalization time between the two groups of electrons was longer than the required time for electrons to leave the cathode fall region. Therefore, electrons have no chance to redistribute themselves in one Maxwellian distribution group. In the positive column region, only one group of electron was detected. Unlike the cathode fall and negative glow regions, the thermalization time was short enough for electrons to redistribute themselves in one Maxwellian distribution group.

If a magnetic field is present in the plasma, it causes helical paths for charged particles around the lines of magnetic force. The radius of the helix decreases with increasing magnetic field. In most circumstances only the paths of electrons are altered, the ions being virtually unaffected. The electrons thus move a much longer total distance in the gas in the order to move a given distance in the direction of the electric field. They hit gas atoms more often and thus have a greater chance of ionization, then the electron temperature decreased more than those in the absence of the magnetic field.

Finally, we note that the electric field distribution increases in the presence of the magnetic field than in the absence due to the increase of the potential distribution, then more excitation and ionization processes occur in a small region, so the plasma density increase more than those in the absence of the magnetic field specially at C.F. and N.G. (due to magnetic field can confine the energetic (ionizing) electrons to a small volume near the electrode).

COMPETING INTERESTS

Authors have declared that no competing interests exist.

REFERENCES

1. Chapman B. Glow discharges processes. J. Wiley and Sons, New York; 1980.
2. Galaly AR, Hassouba MA, Rashed UM. Analysis of cylindrical langmuir probe using experiment and different theories. Plasma Physics Report Journal. 2013; 39(3):1.
3. Radmilovic-Radjenovic M, Radjenovic B. The effect of magnetic field on the electrical breakdown characteristics. J. Phys. D: Appl. Phys. 2006;39.
4. Kagan Y, Paskalev Sov KK. Phys. Tech. Phys. 1975;19:1604.
5. Kagan Y, Perel Sov VI. Probe methods in plasma research. Phys. Usp. 1964;6 767.
6. Zhu Ximing, Pu Yikang. Determination of non-maxwellian electron energy distributions in low-pressure plasmas by using the optical emission spectroscopy and a collisional-radiative model. Plasma Science and Technology. 2011;13(3):267.
7. Isola LM, Gómez BJ, Guerra V. J. Phys. D: Appl. Phys. 2010;43:015202.
8. Galaly AR, El Akshar FF. Determination of the cathode fall thickness in the magnetized DC plasma for Argon gas discharge. Phys. Scr. 2013;88:7.
9. Desilva. Plasma diagnostics. University of Maryland; 1991.
10. Bohm. The characteristics of electrical discharge in magnetic fields. Edited by Guthrie A, Wakerling RK, McGraw-Hill, New York; 1949.
11. Galaly AR. Distributions of electron density and electron temperature in magnetized dc discharge. Physical Science International Journal. 2014;4(7):930.
12. Chen FF. Mini-course on plasma diagnostics. IEEE-ICOPS meeting. Jeju, Korea. 2003;27-28.
13. Hutchinson. Principles of plasma diagnostics. Cambridge Univ. Press; 1990.
14. Helmut O. Rucker Introduction to Plasma. Physics Institute of Physics Karl-Franzens-University Graz, Austria P. 1984;13-14.
15. Chen FF. Plasma diagnostic techniques, edited by Huddlestone E, Leonard SL. Academic Press, New York; 1965.
16. Mott-Smith, Langmuir. Studies of electric discharges in gases at low pressures. Gen. Electron. Rev. 1924;27:449.
17. Mott-Smith, Langmuir. The theory of collectors in gaseous discharges. Phys. Rev. 1926;28:727.
18. Schott. Plasma diagnostic. edited by Lochte-Hogreven W; 1968.
19. Kimura T, Leda Y, Ohe K. XXIII ICPIG Touloouse, France; 1997.
20. Godyak VA, Piejak RB, Alexandrovich BM. Probe diagnostics of non-maxwellian plasmas. J. Appl. Phys. 1993;73:3657.

21. Pringle HD, Farvis WE. J. Phys. Rev. 1955;96:536.
22. Heise C, Kock M. Plasma Sources Science and Technology. 1995;4:31.
23. Yasuda HK, Tao WH, Prelas MA. Journal of Vacuum Science & Technology A [Vacuum, Surfaces, and Films]. 1996;14: 2113.

Peer-review history:
The peer review history for this paper can be accessed here:
http://sciencedomain.org/review-history/10583